

Neutrino Model in Left-Right Symmetric Linear Seesaw Augmented with A_4 Modular Group

Raktima Kalita^{1,*} and Mahadev Patgiri^{1,†}

¹Department of Physics, Cotton University, Guwahati, India

September 19, 2024

Abstract

In this work, we have implemented A_4 modular symmetry in the left-right symmetric linear seesaw model. Interestingly, such modular symmetry restricts the proliferation of flavon fields, and as a result, the predictability of the model is enhanced. The fermion sector of the model comprises of quarks, leptons and a sterile fermion in each generation, while the scalar sector consists of Higgs doublets and bidoublets. We investigate numerically various Yukawa coupling co-efficients, the neutrino masses and mixing parameters in our intended model and predictions become consistent with 3σ range of current neutrino oscillation data. We also studied the non-unitarity, effects on lepton flavor violation in our model and evolution of lepton asymmetry to explain the current baryon asymmetry of the universe.

1 Introduction

The neutrino oscillations confirmed in 1998 by the Super-Kamiokande experiment was a watershed in the history of neutrino physics. This indicated that neutrinos are massive and mixing. Interestingly, neutrinos have tiny masses in sub-eV scale, while two mixing angles are large. In Standard Model (SM) of particle physics, neutrinos are massless, so massive neutrinos are the physics beyond SM (BSM). In the standard parametrization of neutrino mass matrix, the neutrino oscillation parameters, viz., three neutrino mixing

*email: phy2091007_raktima@cottonuniversity.ac.in

†email: mahadevpatgiri@cottonuniversity.ac.in

angles (θ_{ij}) and two mass squared differences (Δm_{ij}^2) have been determined in experiments with a good precision and accuracy. However, some important parameters like the Dirac CP violating phase (δ_{CP}) [1, 2], octant degeneracy of atmospheric mixing angle (θ_{23}), neutrino mass hierarchy and absolute neutrino mass scale are yet to determine. As theoretical attempts to understand the experimental results about neutrinos, a number of neutrino mass models, namely, seesaw mechanism [3–5] with its varieties, radiative mass generation models [6, 7] etc. have been proposed in literature. The existence of sterile neutrinos is one of the key features of BSM scenarios. SM gauge singlets, which are right-handed neutrinos that interact with standard active neutrinos through Yukawa interactions, are generally thought of as sterile neutrinos. The sub-eV scale light neutrinos in the canonical seesaw framework are explained by assuming that the mass of right-handed neutrinos is of the order of 10^{15} GeV, which is beyond the scope of present and forthcoming collider experiments. However, some low-scale mechanisms, such as the extended seesaw [8], linear seesaw [9, 10], inverse seesaw [11–13] etc. require neutrino mass to be in the TeV scale to make them experimentally testable.

It is noted that group symmetries play a crucial role in particle physics. In the literature, wide varieties of neutrino mass models using non-abelian discrete flavor symmetries like S_4 , A_4 , A_5 etc. are available [14–18]. The detailed analysis of these mass models and also their phenomenological implications have been attempted. In this platform, the models require extra flavon fields which are generally SM singlets in the process of their symmetry realization. These flavons play a vital role in understanding of the observed pattern of neutrino masses and mixings by virtue of their particular vacuum alignment [19]. However, the proliferation of flavon fields make the model less predictive. Though flavor symmetry is used to constrain mixing angles but except for few scenarios, the neutrino masses remain undetermined. To get rid of flavon fields, an approach of modular invariance [20] has slowly been attracting attentions of a few authors working in neutrino mass models. One of the striking features of this approach is that it may not require flavon fields other than the modulus, which enhances the power of predictability of the model [21].

In the present work, we deal a left-right symmetric linear seesaw model [22] with modular A_4 symmetry instead of a linear seesaw model with modular A_4 symmetry and global symmetry [23, 24]. We will construct the desired neutrino mass matrix in the proposed framework and perform a systematic numerical analysis to predict various neutrino parameters which are compatible with the current neutrino data.

The organization of this paper is as follows. In Sec. 2, the framework of the left-

right symmetric linear seesaw mechanism has been presented. In Sec. 3, there is a brief overview of the modular symmetry and its implications in particle physics. In Sec. 4, we have constructed our model of the neutrino mass matrix using a linear seesaw mechanism with modular A_4 symmetry. In Sec. 5, a detailed numerical analysis has been performed and examined the compatibility of our model predictions of neutrino observables with the current neutrino data. In Sec. 6 and Sec. 7, we have discussed lepton flavor violating processes and leptogenesis in context of our model. In Sec. 8, we briefly discuss on the collider implications for the present model. Finally, in Sec. 9 we have presented the discussion and conclusion of the results of our proposed work.

2 Left-right symmetric linear seesaw model

The left-right symmetric theory has advanced significantly, providing answers to a number of additional questions including the small mass of neutrino and dark matter sector left unaccounted for by the Standard Model. It was first put forth to explain the origin of parity violation in low-energy weak interactions. The left-right symmetric model (LRSM), introduced by Pati and Salam, is an extension of the Standard Model(SM) of particle physics with the following gauge group [25]

$$SU(3)_C \times SU(2)_L \times SU(2)_R \times U(1)_{B-L} \quad (1)$$

where $B - L$ is the difference between baryon number and lepton number.

The quark and lepton contents of the model are given by

$$q_L = \begin{pmatrix} u_L \\ d_L \end{pmatrix} \sim (3, 2, 1, \frac{1}{3}), \quad q_R = \begin{pmatrix} u_R \\ d_R \end{pmatrix} \sim (3, 1, 2, \frac{1}{3}) \quad (2)$$

$$l_L = \begin{pmatrix} \nu_L \\ e_L \end{pmatrix} \sim (1, 2, 1, -1), \quad l_R = \begin{pmatrix} \nu_R \\ e_R \end{pmatrix} \sim (1, 1, 2, -1) \quad (3)$$

There are the following two Higgs doublets and a bidoublet in the scalar sector of LRSM.

$$H_L = \begin{pmatrix} h_L^- \\ h_L^0 \end{pmatrix} \sim (1, 2, 1, -1), \quad H_R = \begin{pmatrix} h_R^+ \\ h_R^0 \end{pmatrix} \sim (1, 1, 2, -1) \quad (4)$$

$$\Phi = \begin{pmatrix} \phi_1^0 & \phi_2^+ \\ \phi_1^- & \phi_2^0 \end{pmatrix} \sim (1, 2, 2, 0) \quad (5)$$

Again the left-right symmetric linear seesaw requires a neutral gauge singlet fermion S in order to produce neutrino masses. Thus, we obtain the Lagrangian for the leptonic sector as follows:

$$-\mathcal{L}_{lepton} = \bar{l}_L Y \Phi l_R + \bar{l}_L Y \tilde{\Phi} l_R + Y \bar{l}_L H_L S + Y \bar{l}_R H_R S + h.c. \quad (6)$$

where $\tilde{\Phi} = \sigma_2 \Phi^* \sigma_2$ and σ_2 is the second Pauli matrix.

After acquiring vevs, the scalars H_L , H_R and Φ can be written as

$$\langle H_L \rangle = \begin{pmatrix} v_L \\ 0 \end{pmatrix}, \quad \langle H_R \rangle = \begin{pmatrix} v_R \\ 0 \end{pmatrix}, \quad \langle \Phi \rangle = \begin{pmatrix} v_1 & 0 \\ 0 & v_2 \end{pmatrix} \quad (7)$$

Thus, the effective 9×9 neutrino mass matrix in the basis (ν_L, ν_R^c, S) becomes

$$M_\nu = \begin{pmatrix} 0 & m_D & m_{LS} \\ m_D^T & 0 & m_{RS} \\ m_{LS}^T & m_{RS}^T & 0 \end{pmatrix} \quad (8)$$

In the above matrix, the μ term is absent because of the introduction of A_4 symmetry. With $m_{LS} \ll m_D < m_{RS}$, the light neutrino mass formula is given by

$$m_\nu = m_D m_{RS}^{-1} m_{LS}^T + \text{transpose} \quad (9)$$

In addition, the other important neutrino parameters, viz., the effective neutrino mass, m_{ee} and the Jarlskog invariant, J_{CP} which are the measure of the neutrinoless double beta decay rate and strength of CP violation respectively, are given by

$$|m_{ee}| = |m_1 \cos^2 \theta_{12} \cos^2 \theta_{13} + m_2 \sin^2 \theta_{12} \cos^2 \theta_{13} e^{i\alpha_{21}} + m_3 \sin^2 \theta_{13} e^{i(\alpha_{31} - 2\delta_{CP})}| \quad (10)$$

$$\begin{aligned} J_{CP} &= \text{Im}[U_{e1} U_{\mu 2} U_{e2}^* U_{\mu 1}^*] \\ &= \sin \theta_{23} \cos \theta_{23} \sin \theta_{12} \cos \theta_{12} \sin \theta_{13} \cos^2 \theta_{13} \sin \delta_{CP} \end{aligned} \quad (11)$$

The detection of the rare events like neutrinoless double beta decay, a lepton number violation process [26] is very challenging and will confirm the Majorana nature of neutrinos. In this context, the ongoing experiments, viz., GERDA and CUORE are having the sensitivity limits for $|m_{ee}|$ to $(102 - 213)$ meV [27] and $(110 - 520)$ meV [28] respectively. The future generation experiments, LEGEND-200 and KamLAND-Zen have their capabilities to provide the sensitivities for $|m_{ee}|$ up to $(35 - 73)$ meV [29] and $(61 - 165)$ meV [30] respectively.

3 Formalism of Modular Symmetry

The concept of modular transformation and its subgroup symmetry was first introduced in a superstring theory to explain the process of compactification of extra dimensions of space. The two dimensional torus can be constructed as R^2 divided by a two dimensional lattice Λ , which is spanned by the vectors $(\alpha_1, \alpha_2) = (2\pi R, 2\pi R\tau)$ with R being real and τ a complex *modulus* parameter [20, 31–33]. Now the same lattice can also be described in another basis,

$$\begin{pmatrix} \alpha'_2 \\ \alpha'_1 \end{pmatrix} = \begin{pmatrix} a & b \\ c & d \end{pmatrix} \begin{pmatrix} \alpha_2 \\ \alpha_1 \end{pmatrix} \quad (12)$$

where a , b , c , and d are integers and satisfy $ad - bc = 1$, the modulus parameter τ transforms as [21]

$$\tau = \frac{\alpha_2}{\alpha_1} \rightarrow \tau' = \frac{\alpha'_2}{\alpha'_1} = \frac{a\tau + b}{c\tau + d} \quad (13)$$

This modular transformation is generated by $S: \tau \rightarrow -1/\tau$ and $T: \tau \rightarrow \tau + 1$ which satisfy $S^2 = I$ and $(ST)^3 = I$. If $T^N = I$ is required, one is left with the finite subgroups Γ_N which are isomorphic to some even permutation groups, particularly, $\Gamma_2 \simeq S_3$, $\Gamma_3 \simeq A_4$, $\Gamma_4 \simeq S_4$, $\Gamma_5 \simeq A_5$ [31]. The holomorphic functions transforming as $f(\tau) \rightarrow (c\tau + d)^k f(\tau)$ under modular transformation in Eqn. (13) are called the modular forms of weight k . It becomes clear that the modular groups $\Gamma_{2,\dots,5}$ can find some interesting applications in understanding flavor structures of quarks and leptons. The advantage of a modular symmetry over a usual discrete flavor symmetry is that the former dictates the Yukawa-like couplings to be the functions of the modulus parameter τ and transform nontrivially under Γ_N , whereas the latter only acts on the fermion and scalar fields. To achieve the dependence of the Yukawa-like couplings on τ , it has been found that the Dedekind η -function in the following, is a good example of this kind [20].

$$\eta(\tau) = q^{\frac{1}{24}} \prod_{n=1}^{\infty} (1 - q^n) \quad (14)$$

$$q \equiv e^{2\pi i \tau} \quad (15)$$

This satisfies

$$\eta(-1/\tau) = \eta(\tau) \sqrt{-i\tau} \quad \eta(\tau + 1) = \eta(\tau) e^{(i\pi/12)} \quad (16)$$

corresponding to aforementioned transformations.

There are some effective neutrino models of modular symmetry investigated in literature which have attracted the attention of many researchers because of its appealing feature of not requiring flavon fields in symmetry realization apart from a complex modulus, τ . The flavor symmetry is broken when τ acquires vacuum expectation value [34], thus a mechanism is required to fix this modulus τ . Now we outline briefly how modular symmetry is implemented. We consider the modular group, $\Gamma(N)$ which when operates on the complex variable τ belonging to the upper-half of the complex plane i.e., $\text{Im}(\tau) > 0$, it transforms as the following [20]:

$$\gamma(\tau) = \frac{a\tau + b}{c\tau + d} \quad (17)$$

where a, b, c, d are integers forming a matrix

$$\gamma = \begin{pmatrix} a & b \\ c & d \end{pmatrix} \quad (18)$$

with determinant, $ad - bc = 1$.

The modular group is always isomorphic to the projective special linear group $PSL(2, Z) = SL(2, Z)/Z_2$, where $SL(2, Z)$ is a 2×2 matrix with determinant unity. The elements S and T with the condition $S^2 = ST^3 = I$ can generate the modular group and their matrix representations are in the following:

$$S = \begin{pmatrix} 0 & 1 \\ -1 & 0 \end{pmatrix}, T = \begin{pmatrix} 1 & 1 \\ 0 & 1 \end{pmatrix} \quad (19)$$

Such generators when operate on τ yield the following transformations:

$$S : \tau \rightarrow -\frac{1}{\tau}, T : \tau \rightarrow \tau + 1 \quad (20)$$

It is interesting that the Yukawa couplings in the framework of modular symmetry can cast as the functions of the complex modulus τ . With the choice of the modular group, the level and weight of modular symmetry determine the number of modular forms. The number of modular forms related to the non-abelian discrete symmetry group to which it is isomorphic is shown in the table below [20].

Table 1: No. of modular forms corresponding to weight $2k$.

N	No. of modular forms	$\Gamma(N)$
2	$k+1$	S_3
3	$2k+1$	A_4
4	$4k+1$	S_4
5	$10k+1$	A_5
6	$12k$	
7	$28k-2$	

In our work, we shall use $\Gamma(3)$, which is isomorphic to the discrete symmetry group A_4 . The three linearly independent modular forms of weight 2 and level-3 are given by

$$Y_1(\tau) = \frac{i}{2\pi} \left[\frac{\eta'(\frac{\tau}{3})}{\eta(\frac{\tau}{3})} + \frac{\eta'(\frac{\tau+1}{3})}{\eta(\frac{\tau+1}{3})} + \frac{\eta'(\frac{\tau+2}{3})}{\eta(\frac{\tau+2}{3})} - \frac{27\eta'(3\tau)}{\eta(3\tau)} \right] \quad (21)$$

$$Y_2(\tau) = \frac{-i}{\pi} \left[\frac{\eta'(\frac{\tau}{3})}{\eta(\frac{\tau}{3})} + \omega^2 \frac{\eta'(\frac{\tau+1}{3})}{\eta(\frac{\tau+1}{3})} + \omega \frac{\eta'(\frac{\tau+2}{3})}{\eta(\frac{\tau+2}{3})} \right] \quad (22)$$

$$Y_3(\tau) = \frac{-i}{\pi} \left[\frac{\eta'(\frac{\tau}{3})}{\eta(\frac{\tau}{3})} + \omega \frac{\eta'(\frac{\tau+1}{3})}{\eta(\frac{\tau+1}{3})} + \omega^2 \frac{\eta'(\frac{\tau+2}{3})}{\eta(\frac{\tau+2}{3})} \right] \quad (23)$$

$$(24)$$

where $\eta(\tau)$ is the Dedekind eta-function, defined in Eqn. (14)

4 Model Framework

Here, we briefly discuss about the framework for left-right symmetric model with linear seesaw mechanism. In this framework, we have introduced A_4 modular group which minimizes the use of multiple flavon fields. Since modular symmetry has been taken into consideration, we provide the particles with modular weights while keeping in mind that though matter multiplets corresponding to the model may have negative modular weights, but we cannot provide negative weights to the modular forms. These weights are assigned in such a way that the sum of the modular weights in each term of the Lagrangian equals zero. Table 2 provides the particle contents and group charges for the model. The group transformation of the Yukawa couplings is non-trivial in this case. Table 3 lists the group charge and modular weight attributed to the Yukawa couplings.

Table 2: Particle contents and group charges for the model.

Fields	$SU(3)_c$	$SU(2)_L$	$SU(2)_R$	$B - L$	A_4	k_I
$l_{L1,2,3}$	1	2	1	-1	$1, 1'', 1'$	-1
l_R	1	1	2	-1	3	-1
S	1	1	1	0	3	-1
Φ	1	2	2	0	1	0
H_L	1	2	1	-1	1	0
H_R	1	1	2	-1	1	0

Table 3: Modular weight attributed to the Yukawa couplings.

Yukawa coupling	A_4	k_I
Y	3	2

4.1 Dirac mass term for light neutrinos

In this model, the left-handed lepton doublets $(l_{Le}, l_{L\mu}, l_{L\tau})$ are transformed as singlet $(1, 1'', 1')$ and the right-handed lepton l_R transformed as triplet under A_4 modular symmetry. The modular weight assigned to them is -1 . The scalar field, i.e., Higgs bidoublet is transformed as singlet under A_4 modular group. Similarly, the yukawa couplings $Y = (Y_1, Y_2, Y_3)$ transforms as triplet under this symmetry and the modular weight is 2.

Now, the Lagrangian for the Dirac mass term is given by

$$\mathcal{L}_D = \bar{l}_L Y \Phi l_R + \bar{l}_L Y \tilde{\Phi} l_R \quad (25)$$

Therefore, the mass matrix is given by

$$m_D = v_D \begin{pmatrix} Y_1 & Y_3 & Y_2 \\ Y_2 & Y_1 & Y_3 \\ Y_3 & Y_2 & Y_1 \end{pmatrix} \quad (26)$$

where v_D is the vev for the Higgs bidoublet.

4.2 Mixing between ν_L and S

Here, the additional left-right gauge singlet neutral fermion S transforms as triplet under A_4 symmetry. The modular weight assigned to it is -1 . Also, the scalar field H_L transformed as singlet under the given symmetry.

The Lagrangian for this mixing can be written as

$$\mathcal{L}_{LS} = \alpha_{LS}(\bar{l}_{Le})_1 H_L(YS)_1 + \beta_{LS}(\bar{l}_{L\mu})_{1''} H_L(YS)_{1'} + \gamma_{LS}(\bar{l}_{L\tau})_{1'} H_L(YS)_{1''} \quad (27)$$

Now, the mass matrix is given by

$$m_{LS} = v_L \begin{pmatrix} \alpha_{LS} & 0 & 0 \\ 0 & \beta_{LS} & 0 \\ 0 & 0 & \gamma_{LS} \end{pmatrix} \begin{pmatrix} Y_1 & Y_3 & Y_2 \\ Y_2 & Y_1 & Y_3 \\ Y_3 & Y_2 & Y_1 \end{pmatrix} \quad (28)$$

where $(\alpha_{LS}, \beta_{LS}, \gamma_{LS})$ are the free parameters and v_L is the vev for the left-handed Higgs doublet.

4.3 Mixing between ν_R and S

In this mixing, the right-handed lepton l_R and sterile fermion S are transformed as triplet in A_4 modular group. The modular weight assigned to them is -1 . The scalar field H_R transformed as singlet under this group.

The Lagrangian for this mixing is given by

$$\mathcal{L} = \alpha_{RS} Y H_R(\bar{l}_R S)_{\text{sym}} + \beta_{RS} Y H_R(\bar{l}_R S)_{\text{anti-sym}} \quad (29)$$

In the above equation, the first and the second term represent the symmetric and anti-symmetric part for the product of $l_R S$, making it a triplet under the A_4 modular group.

The resultant mass matrix is found to be

$$m_{RS} = v_R \left(\frac{\alpha_{RS}}{3} \begin{pmatrix} 2Y_1 & -Y_3 & -Y_2 \\ -Y_3 & 2Y_2 & -Y_1 \\ -Y_2 & -Y_1 & 2Y_3 \end{pmatrix} + \frac{\beta_{RS}}{2} \begin{pmatrix} 0 & Y_3 & -Y_2 \\ -Y_3 & 0 & Y_1 \\ Y_2 & -Y_1 & 0 \end{pmatrix} \right) \quad (30)$$

where $(\alpha_{RS}, \beta_{RS})$ are the free parameters and v_R is the vev for right-handed Higgs doublet. It is important to observe that $\frac{\alpha_{RS}}{3} \neq \frac{\beta_{RS}}{2}$, otherwise the matrix m_{RS} becomes singular, which spoils the purpose of implementing linear seesaw framework.

4.4 Non-unitarity

Here, we briefly examine the non-unitarity of the neutrino mixing matrix U'_{PMNS} . The standard parametrization for U'_{PMNS} takes the form [35]

$$U'_{PMNS} = \left(1 - \frac{1}{2} F F^\dagger \right) U_{PMNS} \quad (31)$$

where U_{PMNS} is the PMNS mixing matrix that diagonalises the light neutrino mass matrix.

In this case, the hermitian matrix F is shown to be approximately $F \equiv m_{RS}^{-1} m_{LR} \approx \frac{v_L}{v_R}$. The mass of the W boson M_W , the Weinberg angle θ_W , various ratios of the fermionic decays of the Z boson and its invisible decay, electroweak universality, CKM unitarity bounds, lepton flavor violations [36], and other experimental results are used to determine the global constraints on non-unitarity parameters [37, 38]. The outcome of the experiment is provided by [39].

$$|FF^\dagger| \leq \begin{bmatrix} 4.08 \times 10^{-5} & 1.65 \times 10^{-5} & 5.19 \times 10^{-5} \\ 1.65 \times 10^{-5} & 3.85 \times 10^{-5} & 5.04 \times 10^{-5} \\ 5.19 \times 10^{-5} & 5.04 \times 10^{-5} & 1.12 \times 10^{-4} \end{bmatrix} \quad (32)$$

In our model, $(\frac{v_L}{v_R})^2 \approx 10^{-4}$ and $|FF^\dagger| \leq 10^{-4}$, which is completely safe for the given non-unitarity bounds stated above.

5 Numerical Analysis

Neutrino mass and mixing

Here, we will perform the numerical analysis for parameters that satisfy the current data on neutrino oscillations [40]. Table 4 provides the neutrino oscillation data for the 3σ range.

Table 4: Current neutrino oscillation parameters from global fits [40]

Oscillation parameters	Normal Ordering		Inverted Ordering	
	Best fit $\pm 1\sigma$	3σ range	Best fit $\pm 1\sigma$	3σ range
$\Delta m_{21}^2/10^{-5}eV^2$	$7.42^{+0.21}_{-0.20}$	$6.82 - 8.04$	$7.42^{+0.21}_{-0.20}$	$6.82 - 8.04$
$ \Delta m_{3l}^2 /10^{-3}eV^2$	$2.510^{+0.027}_{-0.027}$	$2.430 - 2.593$	$-2.490^{+0.026}_{-0.028}$	$-2.574 - -2.410$
θ_{12}°	$33.45^{+0.77}_{-0.75}$	$31.27 - 35.87$	$33.45^{+0.78}_{-0.75}$	$31.27 - 35.87$
θ_{23}°	$42.1^{+1.1}_{-0.9}$	$39.7 - 50.9$	$49.0^{+0.9}_{-1.9}$	$39.8 - 51.6$
θ_{13}°	$8.62^{+0.12}_{-0.12}$	$8.25 - 8.98$	$8.61^{+0.14}_{-0.12}$	$8.24 - 9.02$
δ_{CP}°	230^{+36}_{-25}	$144 - 350$	278^{+22}_{-30}	$194 - 345$

Here, the neutrino mass matrix of Eqn. (9) can be numerically diagonalized by a unitary matrix U , from which the standard relations can be used to obtain the neutrino

mixing angles:

$$\sin^2 \theta_{13} = |U_{13}|^2, \quad \sin^2 \theta_{12} = \frac{|U_{12}^2|}{1 - |U_{13}^2|}, \quad \sin^2 \theta_{23} = \frac{|U_{23}^2|}{1 - |U_{13}^2|} \quad (33)$$

We can choose the following ranges for the free parameters of the model to satisfy the current neutrino oscillation data:

$$\begin{aligned} \text{Re}[\tau] &\in [0.3, 1.8], \quad \text{Im}[\tau] \in [0.75, 2.5], \quad \{\alpha_{LS}, \beta_{LS}, \gamma_{LS}\} \in 10^{-3}[0.1, 1], \\ \alpha_{RS} &\in [1, 5], \quad \beta_{RS} \in [0, 0.001], \quad v_{LS} \in [10^3, 10^4] \text{ eV}, \quad v_{RS} \in [1, 10] \text{ TeV}, \quad \Lambda \in [10, 100] \text{ TeV}. \end{aligned}$$

The relations provided in Eqn. (33) can be used to get the mixing angles for the model. The variations of the sum of neutrino masses (Σm_ν) with the mixing angles $\sin^2 \theta_{13}$, $\sin^2 \theta_{12}$, and $\sin^2 \theta_{23}$ for both normal and inverted ordering are shown in figures 1, 2, and 3, respectively.

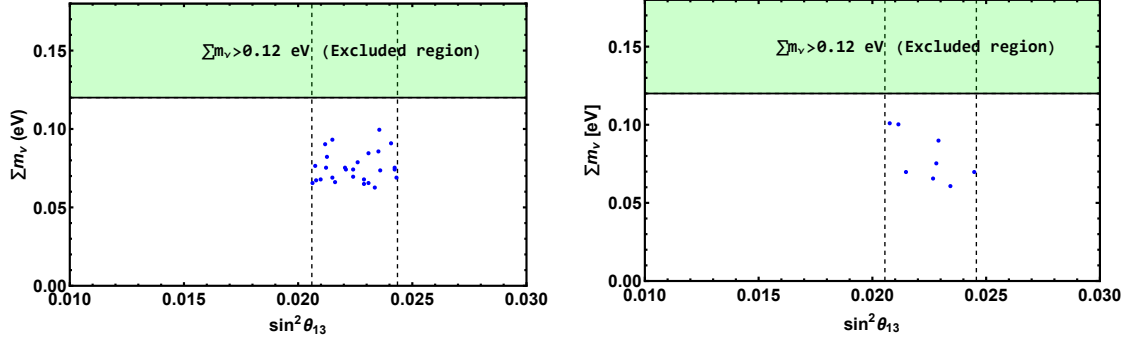


Figure 1: The correlation plot for neutrino masses (Σm_ν) with $\sin^2 \theta_{13}$ for NO (left) and IO (right).

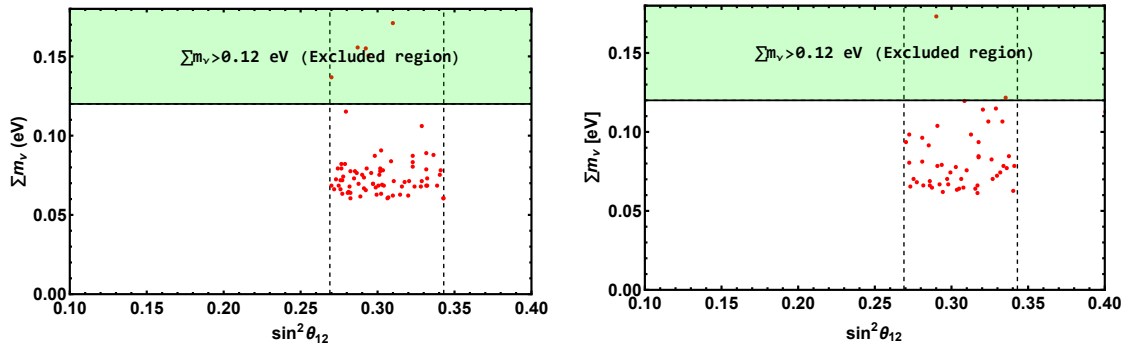


Figure 2: The correlation plot for sum of neutrino masses (Σm_ν) with $\sin^2 \theta_{12}$ for NO (left) and IO (right).

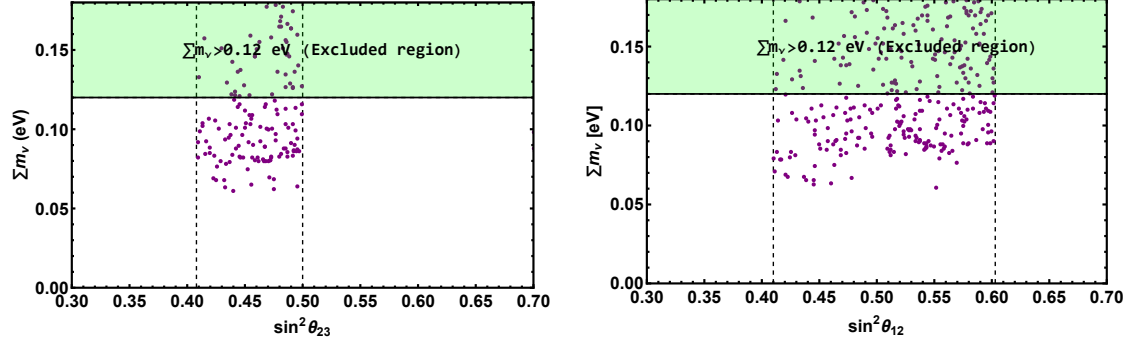


Figure 3: The correlation plot for sum of neutrino masses (Σm_ν) with $\sin^2 \theta_{23}$ for NO (left) and IO (right).

The figures show that a wide range of parameter spaces are within the permitted range for the upper bound of neutrino masses ($\Sigma m_\nu = 0.12$ eV) and the mixing angles. For both NO and IO, the lower bound for the sum of neutrino masses is found to be approximately 0.06 eV.

The correlation between the magnitudes of Yukawa couplings Y_1 and Y_2 , Y_2 and Y_3 are shown in figures 4 and 5 respectively. The ranges for yukawa couplings are given in Table 5.

Table 5: Ranges for Yukawa couplings obtained from the model.

Yukawa couplings	Normal Ordering	Inverted Ordering
$ Y_1 $	0.98 – 1.01	0.90 – 1.05
$ Y_2 $	0.08 – 0.75	0.04 – 1.25
$ Y_3 $	0.002 – 0.26	0.02 – 0.80

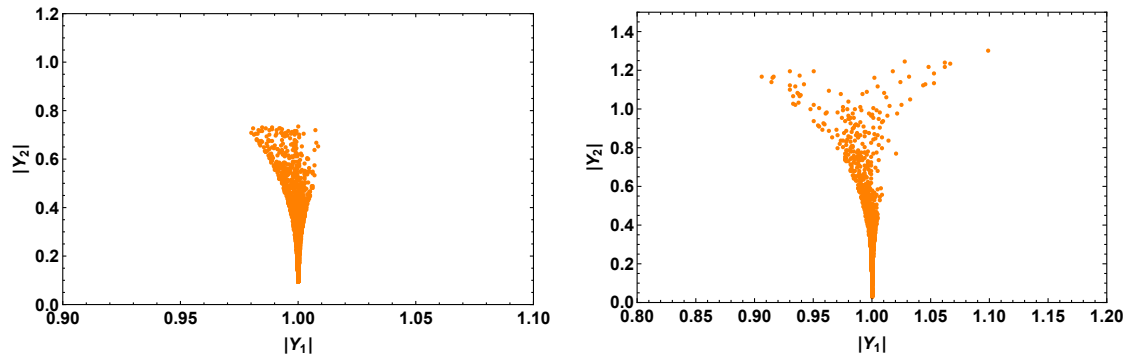


Figure 4: Variation of Yukawa couplings $|Y_1|$ and $|Y_2|$ for NO (left) and IO (right).

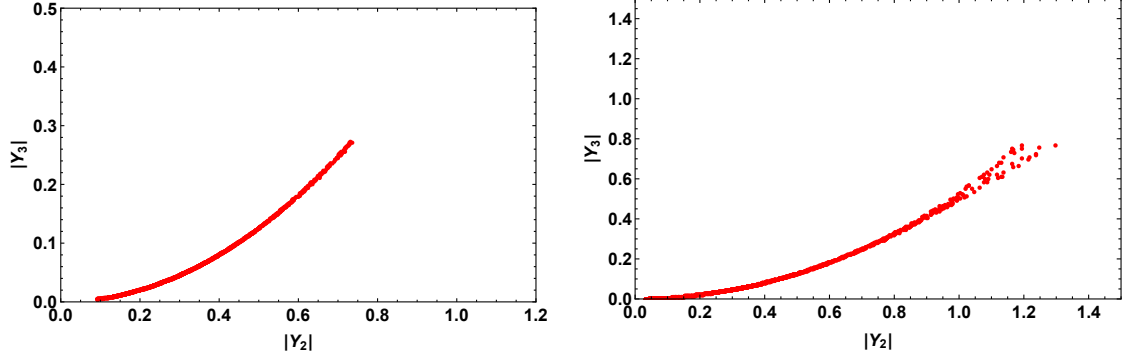


Figure 5: Variation of Yukawa couplings $|Y_2|$ and $|Y_3|$ for NO (left) and IO (right).

The variation between Yukawa couplings and the real component of modulus τ for both NO and IO are shown in figure 6. Furthermore, figure 7 shows the variation of Yukawa couplings with the imaginary component of τ .

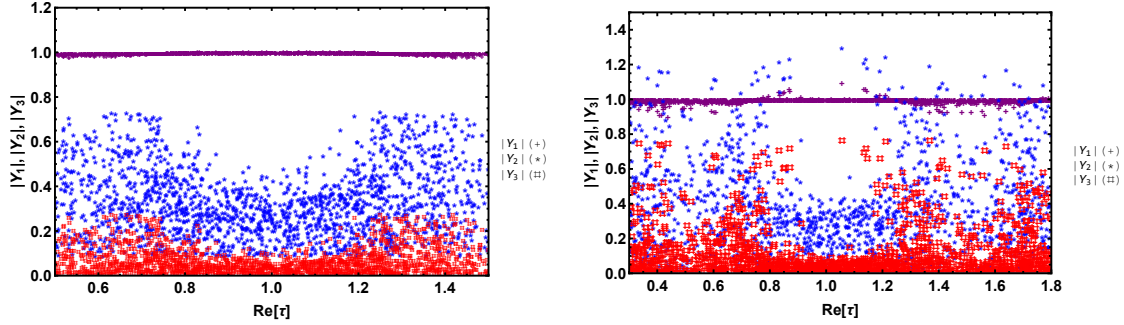


Figure 6: Variation of Yukawa couplings as a function of real component of τ for NO (left) and IO (right).

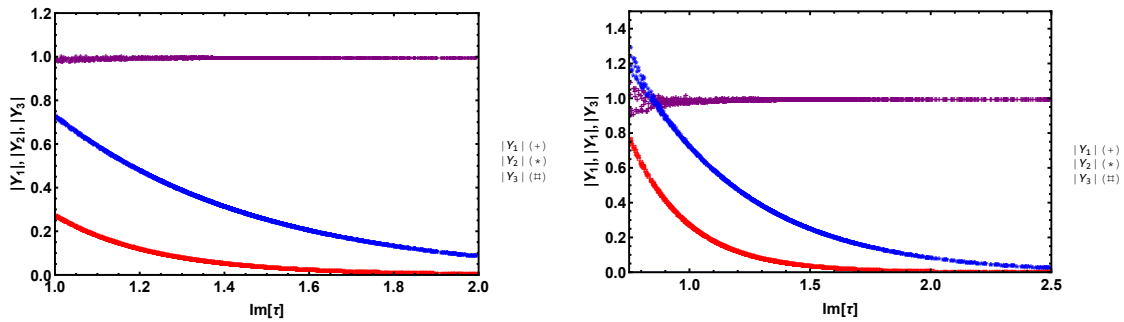


Figure 7: Variation between Yukawa couplings as a function of imaginary component of τ for NO (left) and IO (right).

The region where modulus τ for both NO and IO is allowed and adheres to all the constraints used to deduce the neutrino oscillation parameters is shown in figure 8.

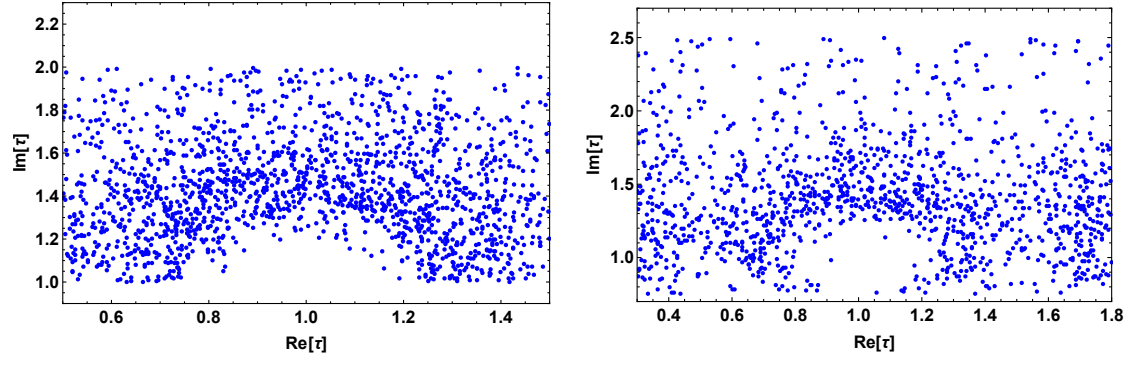


Figure 8: The region of modulus τ satisfying neutrino oscillation data for NO (left) and IO (right).

The parameter space for Yukawa couplings corresponding to the observed sum masses of active neutrinos is shown in figure 9.

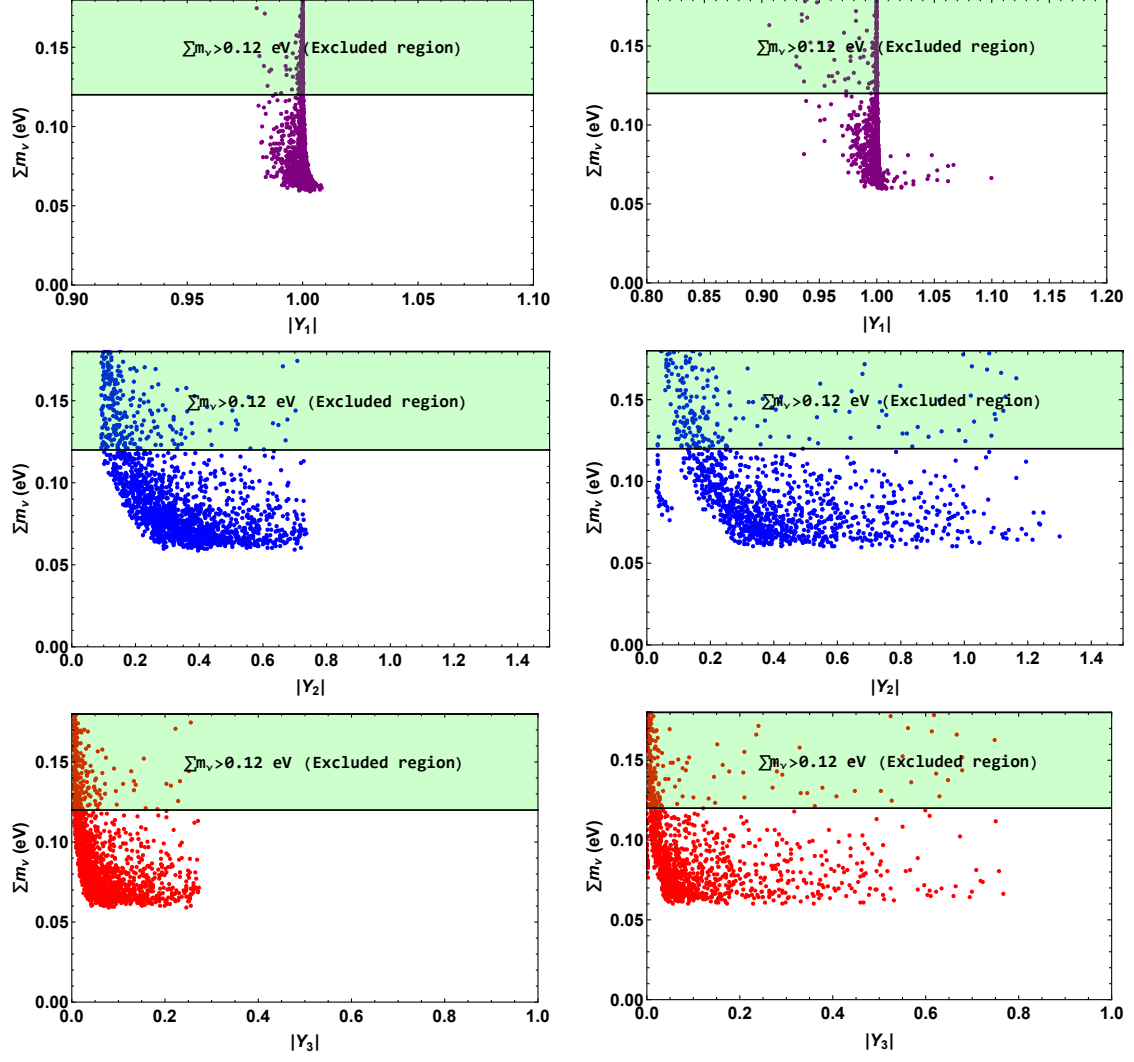


Figure 9: Variation of Yukawa couplings with the sum of active neutrino masses for NO (left) and IO (right).

The correlation between sum of the neutrino masses ($\sum m_\nu$) versus effective mass for neutrinoless double beta decay (m_{ee}) is shown in figure 10.

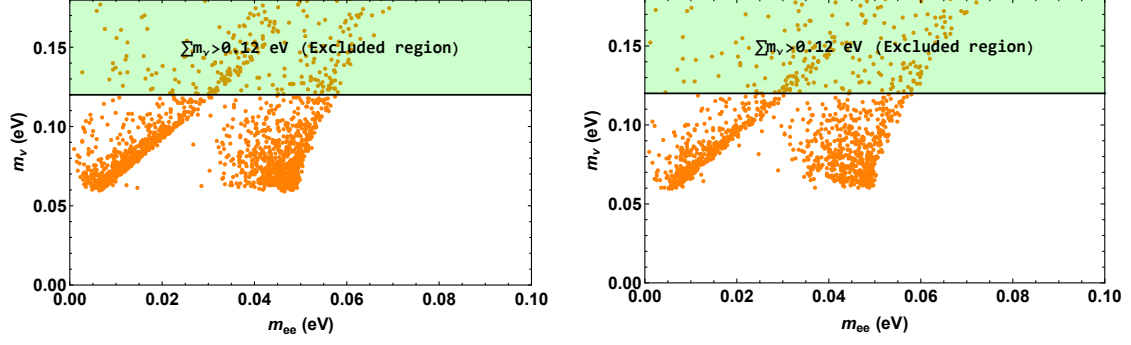


Figure 10: Correlation between sum of neutrino masses ($\sum m_\nu$) versus effective mass for neutrinoless double beta decay (m_{ee}) for NO (left) and IO (right).

From the figure, the effective mass m_{ee} is found to be within the experimental bound for both NO and IO.

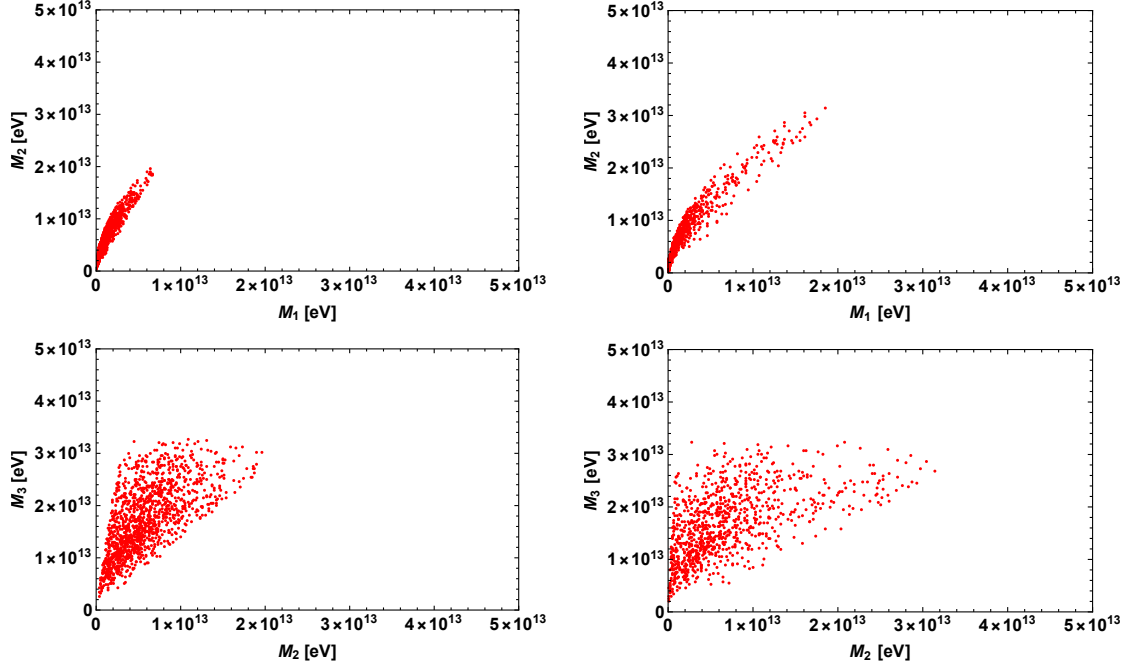


Figure 11: Correlation between the masses of heavy neutrinos for NO (left) and IO (right).

The heavy neutrino masses computed as pseudo Dirac fermions are shown in figure 11. The mass relations are found to be $M_1 \ll M_2 < M_3$ and $M_1 < M_2 \lesssim M_3$ for NO and IO respectively. Additionally, in case of IO, mass scale tends to be larger.

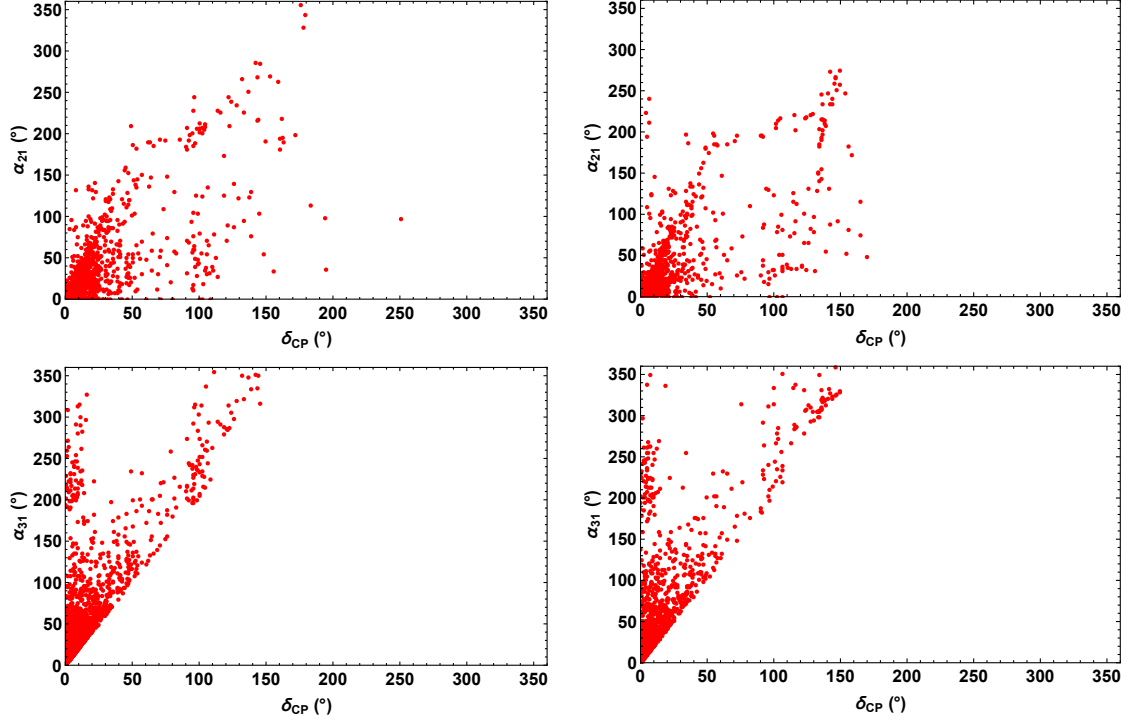


Figure 12: Correlation between Majorana phases and Dirac CP phases for NO(left) and IO(right).

Also, we have calculated Majorana phases for the model. The figure 12 implies that α_{21} takes the value in the range $(0^\circ - 360^\circ)$ for NO and $(0^\circ - 280^\circ)$ for IO. Similarly, the ranges for β are found to be $(0^\circ - 360^\circ)$ for both NO and IO.

The correlation between the Dirac CP phase $\sin^2\theta_{23}$ and the Jarlskog invariant (J_{CP}) is shown in figure 13. The J_{CP} is found to be in the region -0.03 to 0.03 for both normal and inverted orderings.

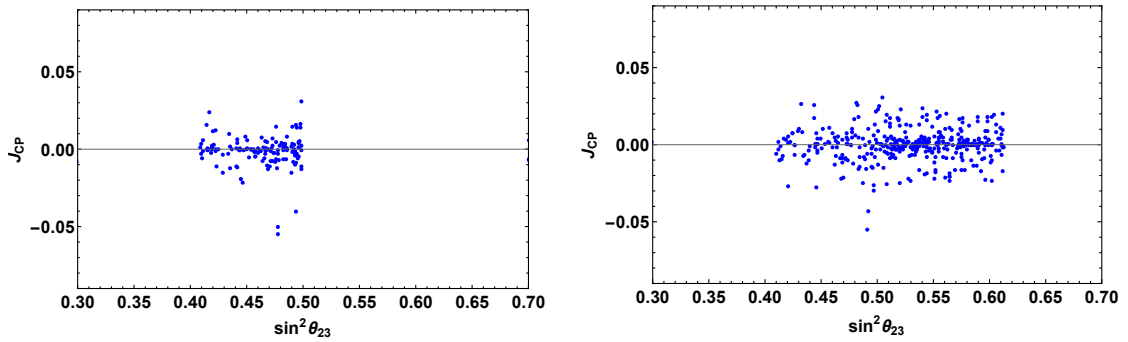


Figure 13: Correlation between Jarlskog invariant (J_{CP}) with Dirac CP phase (δ_{CP}) for NO (left) and IO (right).

6 Lepton flavor violating processes

In the framework of the present model, we will investigate the lepton flavor violation [41] effects on $l_i \rightarrow l_j \gamma$. Lepton flavor violating decays usually forbidden in the Standard Model (SM), however they can be generated through the extension of lepton sector. Based on our model, the Majorana neutrino mass production mechanism can lead to charged LFV. Because $\frac{\Delta m_{21}^2}{m_W^2} \approx 10^{-50}$ is well beyond the sensitivity reach of ongoing and future collider experiments, the GIM mechanism strictly suppresses LFV. However, in the case of a left-right symmetric model, charged LFV might arise as a result of the contribution from heavy right-handed neutrinos. According to the MEG collaboration [42], the current limit on the branching ratios is $\text{BR}(\mu \rightarrow e \gamma) < 4.2 \times 10^{-13}$; for the BABAR collaboration [43], the limit is $\text{BR}(\tau \rightarrow \mu \gamma) < 4.4 \times 10^{-8}$ with 90% confidence level.

The purpose of COMET [44] and Mu2e [45], among other planned experiments, is to achieve the conversion rate for the process $R^N(\mu \rightarrow e)$ in a nucleus [46] at a rate approximately 10^{-17} .

The prediction of Lepton Flavor Violation is affected in our model by unitarity violation. The derivation of various constraints for the model relies significantly on $\mu \rightarrow e \gamma$, as the unitarity violation is of the order of $\frac{m_D^2}{M}$. According to [47], the branching ratio for the process $\mu \rightarrow e \gamma$ is

$$\text{BR}(\mu \rightarrow e \gamma) = \frac{3\alpha}{32\pi} \sum_{i=1}^3 f\left(\frac{M_i^2}{m_W^2}\right) |F_{\mu i}^* F_{ei}|^2 \quad (34)$$

where M_i denotes the physical masses for pseudo-Dirac particles.

Figure 14 shows the Branching ratio for the process $\text{BR}(\mu \rightarrow e \gamma)$ for NO and IO.

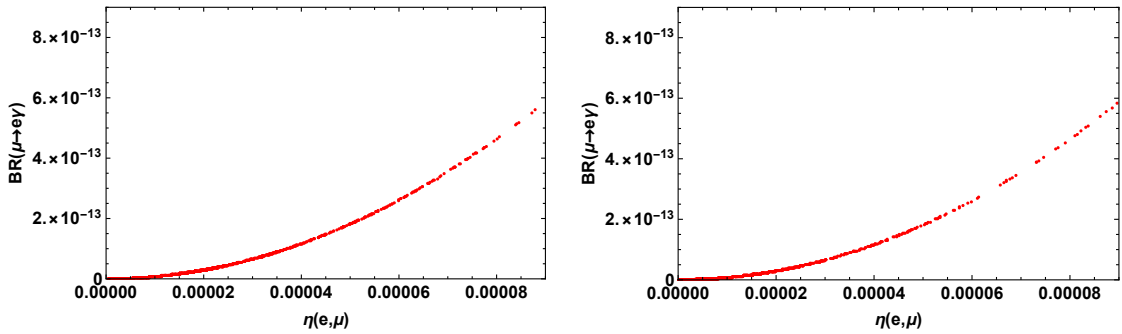


Figure 14: Left and right panels represent the variation of $\text{BR}(\mu \rightarrow e \gamma)$ with $\eta(e, \mu)$ for NO(left) and IO(right).

The branching ratio for the process $\mu \rightarrow e \gamma$ is below 6×10^{-13} for both NO and IO, which is within the current experimental reach, as shown in figures 14.

7 Leptogenesis in the present model

The observed baryon asymmetry of the universe (BAU), which is determined to be $\eta_B^{\text{obs}} = 6.1 \times 10^{-10}$ [48], can be best explained through leptogenesis. It is closely related to the seesaw mechanism involving the violation of lepton number due to right-handed Majorana neutrinos. A very high right-handed neutrino mass of the order 10^{9-14} GeV [49–51] is required for the standard thermal leptogenesis [52] process, and this mass is beyond the scope of current collider experiments. However, this scale has been lowered to the TeV range via resonant leptogenesis [53–55], where heavy neutrinos are quasi-degenerate and their mass splitting is of the order of their decay rates.

The heavy quasi-Dirac pairs in our model have a negligibly small mass splitting, which hinders the generation of the necessary lepton asymmetry. Therefore, the right-handed neutrinos need to have a small Majorana mass M_R in order to generate the necessary mass splitting. Now, the Lagrangian for Majorana mass term can be obtained by

$$\mathcal{L}_R = \alpha_R Y S S \frac{H_R^4}{\Lambda^3} \quad (35)$$

For the right-handed Majorana term, the mass matrix is constructed as

$$M_R = \frac{\alpha_R v_R^4}{3\Lambda^3} \begin{pmatrix} 2Y_1 & -Y_3 & -Y_2 \\ -Y_3 & 2Y_2 & -Y_1 \\ -Y_2 & -Y_1 & 2Y_3 \end{pmatrix} \quad (36)$$

Now, the 2×2 submatrix of Eqn. (8) can be written in the basis (ν_R^c, S) as

$$\begin{pmatrix} 0 & m_{RS} \\ m_{RS}^T & M_R \end{pmatrix} \quad (37)$$

The unitary matrix $\frac{1}{\sqrt{2}} \begin{pmatrix} I & -I \\ I & I \end{pmatrix}$ can be used to construct a block diagonal structure for the matrix given in Eqn. (33) as

$$M' = \begin{pmatrix} m_{RS} + \frac{M_R}{2} & -\frac{M_R}{2} \\ -\frac{M_R}{2} & -m_{RS} + \frac{M_R}{2} \end{pmatrix} \approx \begin{pmatrix} m_{RS} + \frac{M_R}{2} & 0 \\ 0 & -m_{RS} + \frac{M_R}{2} \end{pmatrix} \quad (38)$$

Thus, N_R and S are related to the mass eigenstates (N_{\pm}) by

$$\begin{pmatrix} S_i \\ N_{Ri} \end{pmatrix} = \begin{pmatrix} \cos \theta & -\sin \theta \\ \sin \theta & \cos \theta \end{pmatrix} \begin{pmatrix} N_i^+ \\ N_i^- \end{pmatrix}$$

Assuming maximal mixing, we can write

$$N_{Ri} = \frac{N_i^+ + N_i^-}{\sqrt{2}}, \quad S_i = \frac{N_i^+ - N_i^-}{\sqrt{2}}$$

As a result, the Lagrangian interaction can be modified and expressed in the new basis as

$$\begin{aligned} \mathcal{L}_{LS} = & \alpha_{LS}(\bar{l}_{Le})_1 H_L \left[Y \left(\frac{N_i^+ - N_i^-}{\sqrt{2}} \right) \right]_1 + \beta_{LS}(\bar{l}_{L\mu})_{1''} H_L \left[Y \left(\frac{N_i^+ - N_i^-}{\sqrt{2}} \right) \right]_{1'} \\ & + \gamma_{LS}(\bar{l}_{L\tau})_{1'} H_L \left[Y \left(\frac{N_i^+ - N_i^-}{\sqrt{2}} \right) \right]_{1''} \end{aligned} \quad (39)$$

Now, the modified mass matrix is given by

$$m_{RS} \pm \frac{M_R}{2} = \left(\frac{\alpha_{RS} v_{RS}}{3} \pm \frac{\alpha_R v_R^4}{6\Lambda^3} \right) \begin{pmatrix} 2Y_1 & -Y_3 & -Y_2 \\ -Y_3 & 2Y_2 & -Y_1 \\ -Y_2 & -Y_1 & 2Y_3 \end{pmatrix} \quad (40)$$

Through $(M^\pm)_{diag} = U_{TBM} U_R (M_{RS} \pm \frac{M_R}{2}) U_R^T U_{TBM}^T$, the aforementioned matrix can be diagonalised and the mass eigenvalues are found to be

$$\begin{aligned} M_1^\pm &= \frac{1}{2} \left(\frac{\alpha_{RS} v_{RS}}{3} \pm \frac{\alpha_R v_R^4}{6\Lambda^3} \right) \left(Y_1 + Y_2 + Y_3 + \sqrt{9Y_1^2 - 6Y_1Y_2 + 3Y_2^2 - 2Y_1Y_3 + 3Y_3^2} \right) \\ M_2^\pm &= \frac{1}{2} \left(\frac{\alpha_{RS} v_{RS}}{3} \pm \frac{\alpha_R v_R^4}{6\Lambda^3} \right) \left(Y_1 + Y_2 + Y_3 - \sqrt{9Y_1^2 - 6Y_1Y_2 + 3Y_2^2 - 2Y_1Y_3 + 3Y_3^2} \right) \\ M_3^\pm &= \frac{1}{2} \left(\frac{\alpha_{RS} v_{RS}}{3} \pm \frac{\alpha_R v_R^4}{6\Lambda^3} \right) (Y_1 + Y_2 + Y_3) \end{aligned}$$

Now, the CP asymmetry can be expressed as [54, 56]

$$\epsilon_{N_i^-} \approx \frac{1}{32\pi^2 A_{N_i^-}} \text{Im} \left[\left(\frac{\tilde{m}_D}{v_u} - \frac{\tilde{m}_{LS}}{v_u} \right)^\dagger \left(\frac{\tilde{m}_D}{v_u} + \frac{\tilde{m}_{LS}}{v_u} \right)^2 \left(\frac{\tilde{m}_D}{v_u} - \frac{\tilde{m}_{LS}}{v_u} \right)^\dagger \right]_{ii} \frac{r_N}{r_N^2 + 4A_{N_i^-}^2} \quad (41)$$

where $\tilde{m}_D = m_D U_{TBM} U_R$, $\tilde{m}_{LS} = m_{LS} U_{TBM} U_R$ and r_N and A_N^- are given by

$$r_N = \frac{(M_i^+)^2 - (M_i^-)^2}{M_i^+ M_i^-} = \frac{\Delta M (M_i^+ + M_i^-)}{M_i^+ M_i^-}, \quad A_{N^-} \approx \frac{1}{16\pi} \left[\left(\frac{\tilde{m}_D}{v_u} - \frac{\tilde{m}_{LS}}{v_u} \right) \left(\frac{\tilde{m}_D}{v_u} + \frac{\tilde{m}_{LS}}{v_u} \right) \right]_{ii} \quad (42)$$

Here, $\Delta M = M_i^+ - M_i^- \approx M_R$.

Because modular symmetry is imposed, eliminating extra flavon fields, CP asymmetry parameter of the model greatly relies on the Yukawa couplings in addition to other free

parameters. The dynamics of Boltzmann equations describes the evolution of lepton asymmetry. Now, in order to implement the Sakharov conditions [57], one requires

$$K = \frac{\Gamma_{N_1^-}}{H(T = M_1^-)}$$

where $H = \frac{1.66\sqrt{g_*}T^2}{M_{Pl}}$ with $g_* = 106.75$ and $M_{Pl} = 1.22 \times 10^{19}$ GeV.

Now, the Boltzmann equations are given by [58–61],

$$\begin{aligned} \frac{dY_{N^-}}{dz} &= -\frac{z}{sH(M_1^-)} \left[\left(\frac{Y_{N^-}}{Y_{N^-}^{eq}} - 1 \right) \gamma_D + \left(\left(\frac{Y_{N^-}}{Y_{N^-}^{eq}} \right)^2 - 1 \right) \gamma_s \right], \\ \frac{dY_{B-L}}{dz} &= -\frac{z}{sH(M_1^-)} \left[\epsilon_{N^-} \left(\frac{Y_{N^-}}{Y_{N^-}^{eq}} - 1 \right) \gamma_D - \frac{Y_{B-L}}{Y_l^{eq}} \frac{\gamma_D}{2} \right], \end{aligned} \quad (43)$$

where s denotes the entropy density, $z = \frac{M_1^-}{T}$. Also, the equilibrium number densities can be written as [52]

$$Y_{N^-}^{eq} = \frac{45g_{N^-}}{4\pi^4g_*} z^2 K_2(z), \quad Y_l^{eq} = \frac{3}{4} \frac{45\zeta(3)g_l}{2\pi^4g_*} \quad (44)$$

Here, $K_{1,2}$ are the modified Bessel functions, $g_l = 2$ and $g_{N^-} = 2$. The decay rate γ_D can be expressed by the equation

$$\gamma_D = sY_{N^-}^{eq}\Gamma_D$$

where, $\Gamma_D = \Gamma_{N^-} \frac{K_1(z)}{K_2(z)}$. Moreover, γ_s indicates scattering rate of the decaying particle $N_1^- N_1^- \rightarrow \rho\rho$ [62].

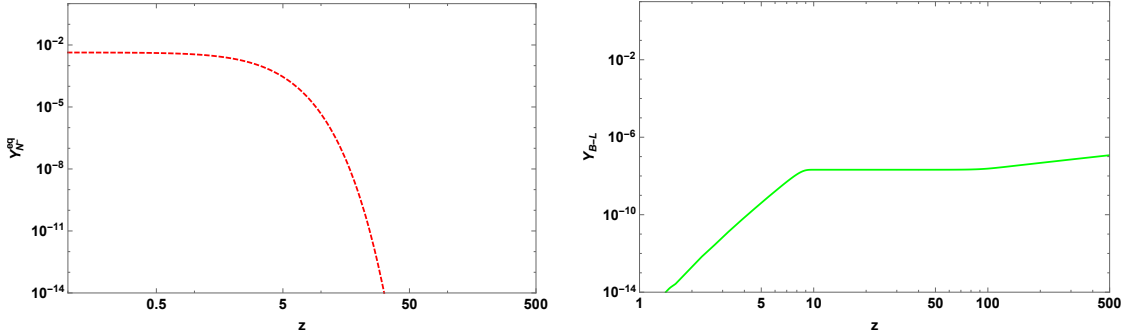


Figure 15: Evolution of $Y_{N^-}^{eq}$ (left) and Y_{B-L} (right) with z .

8 Comment on Collider Physics

Here, we briefly discuss the most promising collider implication of heavy pseudo-Dirac neutrinos within the present model that may be possible at the LHC, without providing

any numerical calculations. Since the M_{LS} is the term that violates the lepton number in the present scenario [63], its mass scale is essentially tiny. Additionally, the effective Majorana neutrino mass matrix for active neutrinos appears in Eqn. (9) where the suppression of the pseudo-Dirac neutrino mass term, M_{LS} , is responsible for the smallness of m_ν . This suppression is further attributed to the ratio of M_D to M_{RS} . Also, trilepton plus missing energy is a significant mechanism involving heavy pseudo-Dirac neutrinos that may be studied at colliders [64, 65].

$$\sigma(pp \rightarrow N l^\pm \rightarrow l^\mp l^\pm + \cancel{E}) = \sigma(pp \rightarrow W \rightarrow N l^\pm) \times Br(N \rightarrow l^\mp l^\pm + \cancel{E}) \quad (45)$$

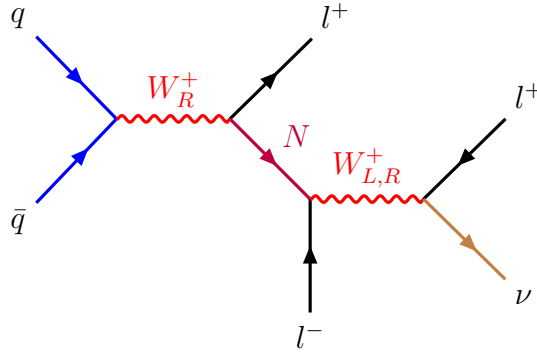


Figure 16: The Feynman diagram showing the decay process for $pp \rightarrow l^+ l^- l^+ \cancel{E}$ process

The possibility of producing this trilepton plus missing energy at the collider is mainly dependent on three factors:

- 1) a significant amount of mixing between heavy pseudo-Dirac neutrinos and light active neutrinos;
- 2) the mass of the heavy neutrinos, ideally ranging from a few [GeV-TeV];
- 3) the method of production of this process.

The only approach available for differentiating between Majorana and pseudo-Dirac neutrinos at the collider is by thorough study of their decay processes. Similarly to the type-I seesaw mechanism, where heavy Majorana neutrinos at the TeV scale, the usual mixing between light-heavy neutrinos is $\theta_{\nu RS} \simeq \sqrt{m_\nu M_{RS}^{-1}} \leq 10^{-6}$ [66].

9 Conclusion

In this study, we have examined a left-right symmetric model enhanced with A_4 modular flavor symmetry, in which the linear seesaw mechanism explains neutrino masses and mix-

ing. This symmetry reduces the use of multiple flavon fields, improving the predictability of the model for both ongoing and upcoming collider experiments. Additionally, the neutrino mass matrix for the model, which is defined by the free parameters and modulus τ , has been constructed.

After that, for both normal and inverted ordering cases, we have performed some numerical analysis to find parameter sets that can fit within the 3σ ranges of neutrino oscillation data. For both NO and IO, the lower bound for the sum of the neutrino masses is around 0.06 eV. Also, the effective mass for neutrinoless double beta decay is found to be within the experimental bound for both NO and IO. Also, the Majorana phase α_{21} takes the value $(0^\circ - 360^\circ)$ for NO and $(0^\circ - 280^\circ)$ for IO. For Majorana phase α_{31} , the range is $(0^\circ - 360^\circ)$ for both NO and IO. Moreover, for both NO and IO, we have determined the J_{CP} of order 10^{-2} . Additionally, the linear seesaw mechanism has been our primary focus since it results in substantial light-heavy neutrino mixing, which is a significant contribution to lepton flavor violating decays such as $\mu \rightarrow e\gamma$, $\mu \rightarrow eee$, and $\mu \rightarrow e$. For the process $\mu \rightarrow e\gamma$, the branching ratio is found to be below 6×10^{-13} for both NO and IO, which can be achieved by the ongoing and upcoming experiments.

We have solved coupled Boltzmann equations with the present set of model parameters to obtain the evolution of lepton asymmetry, which is found to be of the order of $\approx 10^{-8}$. This is sufficient to explain the present baryon asymmetry of the universe. We have also demonstrated that the hierarchy of heavy neutrino mass is $M_1 \ll M_2 < M_3$ for NO and $M_1 < M_2 \lesssim M_3$ for IO. Moreover, we have discussed about the implications of our model in collider physics, where the model may be tested in upcoming experiments.

References

- [1] R Acciarri, MA Acero, M Adamowski, C Adams, P Adamson, S Adhikari, Z Ahmad, CH Albright, T Alion, E Amador, et al., Long-baseline neutrino facility (LBNF) and deep underground neutrino experiment (DUNE) conceptual design report, volume 4 the DUNE detectors at LBNF, *arXiv preprint arXiv:1601.02984*, 2016.
- [2] Constraint on the matter–antimatter symmetry-violating phase in neutrino oscillations. *Nature*, 580(7803):339–344, 2020.
- [3] Peter Minkowski. $\mu \rightarrow e\gamma$ at a rate of one out of 10^9 muon decays? *Physics Letters B*, 67(4):421–428, 1977.

- [4] Rabindra N Mohapatra and Goran Senjanović. Neutrino mass and spontaneous parity nonconservation. *Physical Review Letters*, 44(14):912, 1980.
- [5] Schechter, J and Valle, José WF. Neutrino masses in $SU(2) \otimes U(1)$ theories *Physical Review D*, 22(9):2227, 1980.
- [6] A Zee. A theory of lepton number violation and neutrino Majorana masses. *Physics Letters B*, 93(4):389–393, 1980.
- [7] KS Babu. Model of “calculable” Majorana neutrino masses. *Physics Letters B*, 203(1-2):132–136, 1988.
- [8] Mohapatra, RN and Antusch, S and Babu, KS and Barenboim, Gabriela and Chen, Mu-Chun and De Gouvêa, A and De Holanda, P and Dutta, B and Grossman, Y and Joshipura, A and others. Theory of neutrinos: a white paper. *Reports on Progress in Physics*, 70(11):1757, 2007.
- [9] Malinskỳ, M and Romao, JC and Valle, JWF. Supersymmetric $SO(10)$ seesaw mechanism with low B-L scale. *Physical review letters*, 95(16):161801, 2005.
- [10] Dib, Claudio O and Moreno, Gastón R and Neill, Nicolás A. Neutrinos with a linear seesaw mechanism in a scenario of gauged B-L symmetry. *Physical Review D*, 90(11):113003, 2014.
- [11] M Concepción González-García and José WF Valle. Fast decaying neutrinos and observable flavour violation in a new class of majoron models. *Physics Letters B*, 216(3-4):360–366, 1989.
- [12] AE Cárcamo Hernández, Juan Marchant González, and Ulises Jesus Saldaña-Salazar. Viable low-scale model with universal and inverse seesaw mechanisms. *Physical Review D*, 100(3):035024, 2019.
- [13] Brdar, Vedran and Smirnov, Alexei Yu. Low scale left-right symmetry and naturally small neutrino mass. *Journal of High Energy Physics*, 2019(2):1–29, 2019.
- [14] Brahmachari, Biswajoy and Choubey, Sandhya and Mitra, Manimala. A_4 flavor symmetry and neutrino phenomenology. *Physical Review D*, 77(7):073008, 2008.
- [15] Mukherjee, Ananya and Das, Mrinal Kumar. Neutrino phenomenology and scalar Dark Matter with A_4 flavor symmetry in Inverse and type II seesaw. *Nuclear Physics B*, 913:643–663, 2016.

- [16] Di Iura, Andrea and López-Ibáñez, ML and Meloni, Davide. Neutrino masses and lepton mixing from A_5 and CP. *Nuclear Physics B*, 949:114794, 2019.
- [17] Ma, Ernest. Neutrino mass matrix from S_4 symmetry. *Physics Letters B*, 632(2–3):352–356, 2006.
- [18] Chakraborty, Mainak and Krishnan, R and Ghosal, Ambar. Predictive S_4 flavon model with TM1 mixing and baryogenesis through leptogenesis. *Journal of High Energy Physics*, 2020(9):1–48, 2020.
- [19] Pakvasa, Sandip and Sugawara, Hirotaka. Discrete symmetry and Cabibbo angle. *Physics Letters B*, 73(1):61–64, 1978.
- [20] Feruglio, Ferruccio. Are neutrino masses modular forms? *From My Vast Repertoire... Guido Altarelli's Legacy*, 227–266, 2019.
- [21] Xing, Zhi-zhong. Flavor structures of charged fermions and massive neutrinos. *Physics Reports*, 854:1–147, 2020.
- [22] Sahu, Purushottam and Patra, Sudhanwa and Pritimita, Prativa. A_4 realization of left-right symmetric linear seesaw. *arXiv preprint arXiv:2002.06846*, 2020.
- [23] Behera, Mitesh Kumar and Mishra, Subhasmita and Singirala, Shivaramakrishna and Mohanta, Rukmani. Implications of A_4 modular symmetry on neutrino mass, mixing and leptogenesis with linear seesaw. *Physics of the Dark Universe*, 36:101027 2022.
- [24] Nomura, Takaaki and Okada, Hiroshi. A linear seesaw model with A_4 modular flavor and local $U(1)_{B-L}$ symmetries. *Journal of Cosmology and Astroparticle Physics*, 2022(09):049 2022.
- [25] Grimus, Walter. Introduction to left-right symmetric models. *Vienna Univ.(Austria). Inst. fuer Theoretische Physik*, 2022.
- [26] Schechter, J and Valle, José WF. Neutrino decay and spontaneous violation of lepton number. *Physical Review D*, 25(3):774 1982.
- [27] Agostini, M and Bakalyarov, AM and Balata, M and Barabanov, I and Baudis, L and Bauer, C and Bellotti, E and Belogurov, S and Bettini, A and Bezrukov, L and others. Probing Majorana neutrinos with double- β decay. *Science*, 365(6460):1445–1448 2019.

- [28] Alduino, Chris and Alessandria, F and Alfonso, K and Andreotti, E and Arnaboldi, C and Avignone III, FT and Azzolini, O and Balata, M and Bandac, I and Banks, TI and others. First Results from CUORE: A Search for Lepton Number Violation via $0\nu\beta\beta$ Decay of Te-130. *Physical review letters*, 120(13):132501 2018.
- [29] Giuliani, A and Cadenas, JJ and Pascoli, S and Previtali, E and Saakyan, R and Sch  ffner, K and Schoenert, S. Double beta decay APPEC committee report. *arXiv preprint arXiv:1910.04688*, 2019.
- [30] Gando, Azusa and Gando, Y and Hachiya, T and Hayashi, A and Hayashida, S and Ikeda, H and Inoue, K and Ishidoshiro, K and Karino, Y and Koga, M and others. Search for Majorana neutrinos near the inverted mass hierarchy region with KamLAND-Zen. *Physical review letters*, 117(8):082503 2016.
- [31] de Adelhart Toorop, Reinier and Feruglio, Ferruccio and Hagedorn, Claudia. Finite modular groups and lepton mixing. *Nuclear Physics B*, 117(8):082503 2016.
- [32] Kobayashi, Tatsuo and Tanaka, Kentaro and Tatsuishi, Takuya H. Neutrino mixing from finite modular groups. *Physical Review D*, 858(3):437–467, 2012.
- [33] Kobayashi, Tatsuo and Nagamoto, Satoshi and Takada, Shintaro and Tamba, Shio and Tatsuishi, Takuya H. Modular symmetry and non-Abelian discrete flavor symmetries in string compactification. *Physical Review D*, 97(11):116002, 2018.
- [34] King, Simon JD and King, Stephen F. Fermion mass hierarchies from modular symmetry. *Journal of High Energy Physics*, 2020(9):1–30 2020.
- [35] Forero, DV and Morisi, S and Tortola, M and Valle, JWF. Lepton flavor violation and non-unitary lepton mixing in low-scale type-I seesaw. *Journal of High Energy Physics*, 2011(9):1–18 2011.
- [36] Fernandez-Martinez, Enrique and Hernandez-Garcia, Josu and Lopez-Pavon, Jacobo. Global constraints on heavy neutrino mixing. *Journal of High Energy Physics*, 2016(8):1–31 2016.
- [37] Antusch, Stefan and Fischer, Oliver. Non-unitarity of the leptonic mixing matrix: Present bounds and future sensitivities. *Journal of High Energy Physics*, 2014(10):1–30, 2014.
- [38] Blennow, Mattias and Coloma, Pilar and Fernandez-Martinez, Enrique and Hernandez-Garcia, Josu and Lopez-Pavon, Jacobo. Non-unitarity, sterile neutrinos,

- and non-standard neutrino interactions. *Journal of High Energy Physics*, 2017(4):1–26, 2017.
- [39] Agostinho, Nuno Rosa and Branco, GC and Pereira, Pedro MF and Rebelo, MN and Silva-Marcos, JI. Can one have significant deviations from leptonic 3×3 unitarity in the framework of type I seesaw mechanism? *The European Physical Journal C*, 78:1–11 2018.
- [40] Gonzalez-Garcia, Maria Concepcion and Maltoni, Michele and Schwetz, Thomas. NuFIT: three-flavour global analyses of neutrino oscillation experiments. *Universe*, 7(12):459 2021.
- [41] Deppisch, Frank F. Lepton flavour violation and flavour symmetries. *Fortschritte der Physik*, 61(4-5):622–644, 2013.
- [42] MEG collaboration and others. Search for the Lepton Flavour Violating Decay $\mu^+ \rightarrow e^+ \gamma$ with the Full Dataset of the MEG Experiment. *arXiv preprint arXiv:1605.05081*, 2016.
- [43] Aubert, Bernard and Karyotakis, Y and Lees, JP and Poireau, V and Prencipe, E and Prudent, X and Tisserand, V and Tico, J Garra and Grauges, E and Martinelli, M and others. Searches for lepton flavor violation in the decays $\tau^\pm \rightarrow e^\pm \gamma$ and $\tau^\pm \rightarrow \mu^\pm \gamma$. *Physical review letters*, 104(2):021802, 2010.
- [44] Kurup, Ajit. The coherent muon to electron transition (COMET) experiment. *Nuclear Physics B-Proceedings Supplements*, 218(1):38–43, 2011.
- [45] Kutschke, Robert K. The Mu2e Experiment at Fermilab. *AIP Conference Proceedings*, 1182(1):718–721, 2009.
- [46] Cirigliano, V and Kurylov, A and Ramsey-Musolf, MJ and Vogel, P. Lepton flavor violation without supersymmetry. *Physical Review D—Particles, Fields, Gravitation, and Cosmology*, 70(7):075007, 2004.
- [47] Ibarra, Alejandro and Molinaro, E and Petcov, ST. Low energy signatures of the TeV scale seesaw mechanism. *Physical Review D*, 84(1):013005, 2011.
- [48] Aghanim, Nabila and Akrami, Yashar and Ashdown, Mark and Aumont, Jonathan and Baccigalupi, Carlo and Ballardini, Mario and Banday, Anthony J and Barreiro, RB and Bartolo, Nicola and Basak, S and others. Planck 2018 results-VI. Cosmological parameters. *Astronomy & Astrophysics*, 641:A6, 2020.

- [49] Davidson, Sacha and Ibarra, Alejandro. A lower bound on the right-handed neutrino mass from leptogenesis. *Physics Letters B*, 535(1–4):105–177, 2002.
- [50] Dev, PS Bhupal and Millington, Peter and Pilaftsis, Apostolos and Teresi, Daniele. Flavour covariant transport equations: an application to resonant leptogenesis. *Nuclear Physics B*, 886:569–664, 2014.
- [51] Branco, GC and Felipe, R Gonzalez and Rebelo, MN and Serodio, H. Resonant leptogenesis and tribimaximal leptonic mixing with A_4 symmetry. *Physical Review D*, 79(9):093008, 2009.
- [52] Davidson, Sacha and Nardi, Enrico and Nir, Yosef. Leptogenesis. *Physics Reports*, 466(4–5):25–32, 2008.
- [53] Pilaftsis, Apostolos and Underwood, Thomas EJ. Resonant leptogenesis. *Nuclear Physics B*, 692(3):303–345, 2004.
- [54] Pilaftsis, Apostolos. CP violation and baryogenesis due to heavy Majorana neutrinos. *Physical Review D*, 56(9):5431, 1997.
- [55] Abada, Asmaa and Arcadi, Giorgio and Domcke, Valerie and Drewes, Marco and Klaric, Juraj and Lucente, Michele. Low-scale leptogenesis with three heavy neutrinos. *Journal of High Energy Physics*, 2019(1):1–54, 2019.
- [56] Gu, Pei-Hong and Sarkar, Utpal. Leptogenesis with linear, inverse or double seesaw. *Physics Letters B*, 694(3):226–232, 2010.
- [57] Sakharov, Andrei D. Violation of CP-invariance, C-asymmetry, and baryon asymmetry of the Universe. In *The Intermissions. . . Collected Works on Research into the Essentials of Theoretical Physics in Russian Federal Nuclear Center, Arzamas-16*, 694(3):84–87, 1998.
- [58] Buchmüller, Wilfried and Di Bari, Pasquale and Plümacher, Michael. Leptogenesis for pedestrians. *Annals of Physics*, 315(2):305–351, 2005.
- [59] Plümacher, Michael. Baryogenesis and lepton number violation. *Zeitschrift für Physik C Particles and Fields*, 74:(549–559), 1997.
- [60] Giudice, Gian Francesco and Notari, A and Raidal, M and Riotto, A and Strumia, A. Towards a complete theory of thermal leptogenesis in the SM and MSSM. *Nuclear Physics B*, 685(1-3):89–149, 2004.

- [61] Strumia, Alessandro. Baryogenesis via leptogenesis. *Les Houches*, 84:655–680, 2006. *Physical Review D*, 98(1):016004, 2018.
- [62] Iso, Satoshi and Okada, Nobuchika and Orikasa, Yuta. Resonant leptogenesis in the minimal B-L extended standard model at TeV. *Physical Review D*, 83(9):093011, 2011.
- [63] Han, He-chong and Xing, Zhi-zhong. A full parametrization of the 9×9 active-sterile flavor mixing matrix in the inverse or linear seesaw scenario of massive neutrinos. *Nuclear Physics B*, 973:115609, 2021.
- [64] Chen, Chien-Yi and Dev, PS Bhupal. Multilepton collider signatures of heavy Dirac and Majorana neutrinos. *Physical Review D—Particles, Fields, Gravitation, and Cosmology*, 85(9):093018, 2012.
- [65] Das, Arindam and Dev, PS Bhupal and Okada, Nobuchika. Direct bounds on electroweak scale pseudo-Dirac neutrinos from $s = 8$ TeV LHC data. *Physics Letters B*, 735:364–370, 2014.
- [66] Del Aguila, F and Aguilar-Saavedra, JA. Distinguishing seesaw models at LHC with multi-lepton signals. *Nuclear Physics B*, 813(1-2):22–90, 2009.